Experimental investigation of performance reliability of macro fiber composite for piezoelectric energy harvesting applications

Deepesh Upadrashta and Yaowen Yang*

School of Civil and Environmental Engineering, Nanyang Technological University, 50 Nanyang Avenue, 639798, Singapore

*Corresponding author, Email: cywyang@ntu.edu.sg

Abstract

Macro fiber composite (MFC) has been extensively used in actuator/sensor/harvester applications. Fatigue due to cyclic high electric fields in actuator applications has been studied extensively. However, fatigue failure of MFC due to high stress or strains in energy harvesting applications has attracted little attention. The aim of the study is to obtain the upper limit of dynamic strain on MFC which can be used as failure limit in the design process of piezoelectric energy harvesters (PEHs). The examined PEH is comprised of a cantilever beam made of aluminum and a patch of MFC bonded at its root for power generation. Energy harvesting tests are conducted at various base accelerations around 30Hz (near resonant frequency) and the voltage output and maximum strain on MFC are measured. Severe loss in the performance of the harvester is observed within half million cycles of testing at high strain amplitude. Hence several reliability tests for extended periods of time are carried out at various strain amplitudes. The harvesters are tested at resonant frequencies around 30Hz and 135Hz for over 20 million and 60 million cycles, respectively. Degradation in voltage output, change in natural frequency and formation of cracks are considered as failures. Based on the experimental results, an upper limit of 600$\mu\epsilon$ is proposed as the safe amplitude of strain for reliable performance of MFC. Tensile tests are also carried out on MFC patches to understand the formation of cracks and shift in resonant frequency at low strains. It is observed that cracks are formed in MFC at strains as low as 1000$\mu\epsilon$. The observations from this work are also applicable to MFC bending actuators undergoing cyclic strains.

Keywords

Piezoelectricity, energy harvesting, macro fiber composite, reliability, fatigue strength, fatigue, durability

1. Introduction

Over the years, the emphasis on structural health monitoring using wireless sensor nodes, intelligent control systems, sensing systems in smart buildings, low-power portable electronic devices, etc., has been increased. The systems in aforementioned applications are normally powered by chemical batteries that require periodic maintenance and proper disposal of hazardous chemical waste. With continuous reduction in power consumption of electronic circuitry, energy harvesting from ambient sources has emerged as an alternative solution for chemical batteries in low-power electronics and their applications. Vibration energy harvesting using piezoelectric transduction mechanism has received much attention due to its superior power density, ease of application and scalability [1]. In the last decade, piezoelectric energy harvesting has been used in macro, meso, MEMS and nanoscale applications as an alternative clean energy source [2]. A majority of research has focused on using piezoelectric energy harvesters (PEHs) as alternatives to chemical batteries for running low-power electronic devices and wireless sensor nodes (WSNs). The continuous reduction in size and power consumption of electronic devices and ongoing research in efficient power management of circuitry also help in practical implementation of PEHs for powering small scale devices.

Most of the designs of PEHs are linear energy harvesters that generate maximum power at the resonant frequency. Linear energy harvesters have been extensively studied using analytical models with experimental validation [3, 4]. Finite element modeling has also been used for studying the dynamics of the linear harvesters [5, 6]. The limitation of linear PEHs lies in their small half power bandwidth and hence they cannot produce usable power output away from resonant frequency. This issue poses serious challenge when the ambient vibrational energy is scattered over a range of frequency or for the case of random vibrations. Many techniques have been employed to broaden the bandwidth of the linear harvesters, including oscillator arrays, multi-modal oscillators, passive and active resonance tuning and nonlinear techniques [7]. Despite of extensive work, researchers still face many challenges in practical implementation of PEHs. Even if the complete replacement of batteries by PEHs is not possible, the technology can be used for recharging batteries and for extending the lifetime of device.

Structural integrity and reliable performance over extended periods of time are important considerations in design and practical implementation of PEHs. In PEHs, brittle piezoelectric materials are very susceptible to fatigue failure due to the cyclic electromechanical loading on the harvester. Normally, a PEH is comprised of a piezoelectric material bonded to a substrate such as aluminum, brass, steel etc. Strength of some commercially available piezoelectric materials and commonly used substrate materials is given in Table 1. The values represent the strength of materials under various testing conditions such as quasi-static (tensile), fatigue (dynamic), bending, yielding and fracture as notified in supplier's data sheet. The material strength is specified either in $\mu\epsilon$ (micro strain) or MPa (stress). The fatigue strength of the piezoelectric materials which is crucial information required for designing highly durable harvesters is not provided in most of the instances. From the tabulated data, it is conspicuous that the fatigue strength of piezoelectric materials is much less when compared to static and bending strength. Though macro fiber composite (MFC) has very high fracture strength, normally the material fails at much lower strain values under cyclic loading. Moreover, the information on the reliability of performance of materials such as number of cycles without any degradation is not available.

It is also evident from the table that the strength of the commonly used substrate materials is much superior to piezoelectric materials, indicating the possibility of early fatigue failure in piezoelectric materials. However, very few works have taken the material strength into consideration in the design of PEHs. Anton et al. [8] carried out 3-point bending tests on monolithic piezoceramics PZT-5A and PZT-5H, single crystal piezoelectric PMN-PZT and commercially packaged QuickPack devices and reported their strengths to be used as the basis for the design of PEHs. These results are also included in Table 1 and it can be observed that they are among the highest as they are obtained from quasi-static bending tests. However, fatigue strengths are required for the design of harvesters rather than static strengths. Shafer and Garcia [9] derived an expression of the maximum tolerable input acceleration that a linear energy harvester can sustain based on the ultimate strength of the piezoelectric material and used this expression to determine the maximum harvested power corresponding to that acceleration. Deepesh et al. [10] carried out a parametric study to obtain the optimal power output and bandwidth from a nonlinear harvester within allowable limits of strain on the piezoelectric material.

Table 1. Material strength of commonly used piezoelectric and substrate materials

Material	Manufacturer	Product specification	Material strength	
MFC patch	Smart materials	M2807-P2	4500με [fr][i]	
PZT wafer	MIDE Volture	V22BL	800με [b][ii]	
PZT Bimorph	Morgan Advanced Materials	PZT 5A series	75.8MPa [s][iii]	27.6MPa [f][iii]
PZT ceramics	Piezo Systems, Inc.	PSI-5A4E	140.4MPa [b] [8]	
		PSI-5H4E	114.8MPa [b] [8]	
PZT composite	MIDE QuickPack	QP10N	206.4MPa [b] [8]	
PZT patch	Channel Industries, Inc.	PZT 5804 Navy III	82.7MPa [s][iv]	48.3MPa [f][iv]
PMN-PZT	Ceracomp Co., Ltd.	CPSC 160-95	44.9MPa [b] [8]	
Substrate materials				
Aluminum	--	AL 6061 T6	276MPa [y][v]	96.5MPa [f][v]
Brass	--	230 BRASS H08	435MPa [y] [vi]	
Steel	--	AISI 1050 rolled steel	415MPa [y] [vii]	

Note: (1) [s]=static; [f]=fatigue; [b]=bending; [y]=yield; [fr]=fracture (2) The superscripts [i] to [vii] represent the data sources, given at the end of this paper.

The fatigue behavior of piezoelectric materials has been extensively studied in the literature for actuator applications. Lupascu and Rödel [11] studied the microscopic mechanisms causing fatigue phenomenon in bulk PZT actuator materials under cyclic loading. The fatigue behavior of an adaptive structure comprising graphite/epoxy laminate with embedded PZT actuator was investigated by Mall and Hsu [12] for mechanical and electromechanical cyclic loading conditions. Only tensile stresses were applied in both cyclic loading conditions. Significant drop in actuator's voltage was observed within one million cycles and higher voltage drop was noticed as the mechanical stress was increased. A similar study was carried out by Yocum et al. [13] on a composite laminate with embedded piezoelectric actuator under fully reversed electromechanical cyclic loading. Chaplya et al. [14] studied the influence of electro-thermo-mechanical loading conditions on the actuation capabilities of five commercial piezoelectric stack actuators with emphasis on durability performance. Experimental results indicated a strong dependence of piezoelectric properties and power requirements on both mechanical loading and temperature. Wang et al. [15] evaluated the reliability of piezoelectric actuators under high cyclic electric fields with different magnitudes of mechanical preload. The results demonstrated a monotonic decrease in charge density and mechanical strain as loading cycles increased and the degradation was dependent on preload stress. Wang et al. [16] also studied piezoelectric and dielectric performance of a poled PZT subjected to electric cyclic loading conditions similar to high-field actuator applications. Bhattacharyya and Arockiarajan [17] investigated the influence of electrical fatigue on PZT for different loading frequencies and observed appreciable reduction in piezoelectric and dielectric coefficients for high number of cycles. In 2002, NASA Langley Research Center developed MFC which is a low-cost piezo composite actuator with high flexibility [18]. The MFC consists of a single layer of rectangular lead zirconium titanate (PZT) fibers embedded in epoxy matrix and kapton (polyimide) shell and offers high strain energy density, directional actuation, conformability and durability. It was reported that the MFC is capable of enduring large strains about 2000με (peak to peak) up to 100 million cycles without any degradation in free-strain performance. However, approximately 5% degradation in the performance was observed when the MFC was operated under cyclic loading of 1500V (peak to peak), +300V bias at 500 Hz. The MFC has also been used in special applications apart from typical actuators/sensors/harvesters. Tarazaga et al. [19] successfully tested the integration, packaging, deployment and thermal rigidization in vacuum, and operation of MFC in rigidizable inflatable boom application. The MFC was also used in health monitoring of the wing skin-to-spar joints of unmanned aerial vehicles [20].

As pointed out earlier, previous studies have evaluated the fatigue behavior of piezoelectric materials mainly for actuator applications. While strong electric fields are common in actuator applications, piezoelectric materials in PEHs experience high stress or strain fields. Furthermore, they undergo completely reversed cyclic loading, meaning equal amplitude of tensile and compressive strains with zero mean. Previous studies on actuators used either tensile strains or biased voltages which resulted in lower compressive strains. Though bulk piezoceramics exhibit good compressive strength [21], thin or film like patches used in actuators/sensors/harvesters do not have the capability to withstand high compressive loading. Moreover, high durability and structural integrity are required for piezoceramics for practical applications of PEHs. However, neither previous works nor supplier's data sheets provide estimates of material strength below which the piezoelectric materials perform with high reliability over extended periods of time.

In this work, the MFC is tested for reliability of its performance at different strain amplitudes with varied loading frequencies. Three types of experiments are performed for evaluating the performance of MFC. Firstly, energy harvesting tests are carried out with cantilever type PEH to estimate the voltage output and strain on MFC. The results prompted the authors to perform tensile tests on the MFC to understand certain phenomenon observed in the energy harvesting tests. Finally, several long duration tests are conducted with increased strain amplitudes at different frequencies to evaluate the reliability of harvester's performance. Based on the results, a safe dynamic strain limit on the MFC is proposed for reliable operation.

2. Energy harvesting tests

The schematic of PEH is shown in Figure 1(a). The PEH is comprised of a cantilever beam made of aluminum (AL6061 T6) with a patch of MFC (M2807-P2) bonded to its root using DP-460 epoxy glue. A tip mass made of acrylic was attached to the free end of the cantilever beam to tune its resonant frequency. The tip mass has dimensions of 25mmx15mmx10mm and a weight of 7.3g. Strain gauge DSFLA-5-350 of dimensions 5mm x 2mm was bonded on the top of MFC at distance of 2mm from the clamped end. A resistor was connected across MFC to measure the voltage output. The experimental setup of energy harvesting tests is shown in Figure 1(b). The geometric parameters and material properties of the harvester used in experiments are given in Table 2. The PEH was clamped to the shaker arm and the base acceleration was given through the combination of APS shaker (APS 113), waveform generator (ALP1020) and amplifier (APS 125). The Polytec laser vibrometer was used for measuring displacement of the tip mass. Data of base acceleration, voltage, strain and displacement were acquired through high precision NI-DAQ modules. The experiments were conducted at identified optimal resistance of 410kΩ. The frequency sweep tests were conducted at six different base accelerations ranging from $1m/s^2$ to $6m/s^2$.

Table 2. Geometric parameters and material properties of PEH

Parameter	Piezoceramic	Substrate	Epoxy
Material	MFC 2807-P2	Aluminum	DP-460
Length (mm)	28	70	28
Width (mm)	7	10.6	7
Thickness (mm)	0.3	0.67	0.1
Elastic modulus (GPa)	30.336	68.9	2.7
Poisson's ratio	0.31	0.33	0.4
Mass density (kg/m^3)	5440	2700	1100
Piezoelectric constant (C/m^2)	-5.16	---	---
Capacitance (nF)	9.5	---	---
Optimal Resistance (kΩ)	410		
Tip mass (g)	7.3		

Variation of the root mean square voltage (V_{rms}) response of the harvester during frequency sweep for different accelerations is plotted in Figure 2(a). The resonant frequency of the harvester is observed at 31.1Hz for base acceleration of 1m/s^2 and decreases gradually as the base acceleration increases. The resonant frequency is reduced to 30.4Hz for base acceleration of 6m/s^2 and resulting in 0.7Hz of frequency shift. The maximum bending strain on MFC is shown in Figure 2(b). The values indicate the amplitude of strain (either tension or compression) at the root of top layer of MFC. As already pointed out that the strain gauge is 5mm in length and bonded at 2mm from the clamped end, hence the strain is measured at a distance of 4.5mm from the clamped end where the maximum strain is induced. According to Euler-Bernoulli beam theory, variation of bending strain along the length of the beam is proportional to the curvature of the beam. Using the above principle and by evaluating the mode shape of beam, it is determined that the measured strain is approximately 0.93 times of maximum strain at the root for the above beam configuration. Hence, the maximum strain plotted in Figure 2(b) is calculated by dividing the measured strain by 0.93.

The supplier's data sheet indicates 1000με as the linear elastic limit of MFC. However, it is clear from Figure 2(a) and 2(b) that shifts in resonant frequency is observed even from low strain amplitudes. For example, for low accelerations of 1m/s^2 and 2m/s^2, with corresponding maximum strains of 340με and 535με in the MFC, the resonance shifts from 31.1Hz to 30.9Hz. Similar nonlinear behavior in the form of resonant frequency shift is apparent at all the tested excitations, indicating the absence of linear elastic limit for MFC contrast to the supplier's data. Note that the harvester materials experience some mean strain due to the weight of the tip mass. However, the magnitude of induced mean strain is very low and within the range of measuring accuracy of strain gauge (0-75με). Therefore, the mean strain on the PEH due to the weight of tip mass cannot be measured by the strain gauge and thus evaluated using simple finite element static analysis. Finite element model of tested PEH is shown in Figure 3(a) and the evaluated strain on harvester materials is shown in Figure 3(b) with maximum strain of 90με on MFC at the clamped end. Note that, the resistor is not included in finite element analysis as it is a static analysis. The strain gauge reading is normally calibrated to zero before commencing dynamic tests and hence the results in Figure 2(b) indicate only strain amplitudes. Throughout this paper, strain values are rounded to nearest multiples of 5με. The true strain can be calculated by adding the mean strain value to the amplitude. The measured strain amplitude at resonance for the base acceleration $6m/s^2$ is 1370με. Hence, the state of strain on MFC varies between -1280με and 1460με at resonance of $6m/s^2$.

The energy harvesting tests were not conducted at higher base accelerations as the voltage response at resonance corresponding to $6m/s^2$ shows continuous degradation. The response of the harvester was recorded for half million cycles to estimate the performance degradation. In Figure 4(a), the variation of voltage output with the number of cycles is plotted for base acceleration of $6m/s^2$. The resonant frequency was checked approximately after every 25k cycles and the excitation frequency was matched with the new resonant frequency. Essentially, the harvester was tuned to vibrate at its resonant frequency throughout the tested period of 0.5 million cycles. The strain on MFC and resonant frequency are plotted in Figure 4(b). It can be observed that the voltage output is reduced to 50% within 0.25 million cycles of operation which is about 2.5hours. The resonant frequency is also reduced, indicating decrease in beam stiffness possibly due to excessive deformation or cracking in MFC or debonding between PZT fibers and epoxy matrix. The sudden rise in strain on MFC between 0.2 and 0.35 million cycles indicates possible failure of MFC. The sharp reduction in voltage output can also be observed during that interval in Figure 4(a). It is worth mentioning that the loss in performance of harvester is not due to fatigue under electrical loading but solely because of fatigue due to alternating bending strain. Assuming a uniform electric potential across the PZT layer of 0.18mm thickness in MFC, the maximum value of induced electric field in the MFC is 0.29kV/mm only. This induced electric field in PEH is much lower as compared to actuator applications. Hence, the performance degradation in MFC due to cyclic electrical loading can be neglected. These results show that the MFC cannot withstand high strains for a long period of time. To better understand the nonlinear behavior of MFC (resonance shift) and to examine its failure limit, tensile tests were carried out and details are presented in the next section.

3. Tensile tests of macro fiber composite

Tensile tests were carried out on MFC-P2 specimens to understand the nonlinear behavior and to obtain the failure limit. The dimensions of the tested MFC specimen were 85mm x 7mm x 0.3mm. The gauge length between the grips of tensile testing machine was kept to 28mm similar to the length of MFC used for PEH in energy harvesting tests (see Table 2). A strain gauge (DSFLA-5-350) was attached to the middle portion of the specimen and the strain was measured using the NI-9237 data acquisition module. The MFC with bonded strain gauge is shown in Figure 5(a). Each MFC was tested using the MTS C-42 tensile testing machine with high accuracy load cell and screw grips. The specimens were loaded at crosshead speed of 0.1mm/min up to strain of 4500με which is given as the maximum limit by the supplier.

The stress-strain behavior obtained from the tensile tests on five specimens is plotted in Figure 6(a). The stress is calculated by dividing the applied force with the cross sectional area of MFC specimen ($2.1mm^2$). A polynomial fit is constructed using the MATLAB curve fitting tool box from the experimental data. The nonlinear stress-strain behavior in polynomial form is mathematically convenient to include the material nonlinearity in analytical models of dynamic systems. Some publications in piezoelectric energy harvesting have also used high order polynomials to represent the material and damping nonlinearities [22-23]. The slope of the polynomial fit which represents the variation of elastic modulus with strain is plotted in Figure 6(b). The important feature that can be observed from Figure 6(a) and 6(b) in the context of present study is the nonlinearity in stress-strain behavior for lower strains (e.g. <1000με). Though some deviation in material behavior is observed from specimen to specimen, the overall trend confirms the nonlinearity at lower strains. The elastic modulus decreases by approximately 55%

between 0 to 1000με due to material nonlinearity and this explains the resonant frequency shift observed in the energy harvesting tests. Note that the wavy trend of elastic modulus beyond 1500με is due to the inherent oscillatory nature of polynomial fit.

Williams et al. [24] performed material testing on the MFC, fitted the experimental data using the Ramberg-Osgood model and proposed 1000με as the linear elastic limit for MFC by ignoring the slight nonlinearity below 1000με. They used the MFCs of larger dimensions (88.9mm x 25.4mm x 0.302mm) and higher strain rate (0.2mm/min) for testing. Their results showed a higher ultimate stress of 43MPa, while the MFCs in our tests could withstand only 36.5MPa. The lower strain rate (0.1mm/min) used in the present study might have resulted in gradual application of load and therefore helped in obtaining nonlinear behavior. Moreover, the 1000kN load cell was used in Williams et al.'s study where the maximum applied load on MFC is just about 0.035% (350N) of the capacity of load cell. The accuracy of load cell in reading such a small applied load is questionable. In our experiment, a high accuracy 250N load cell is used and the maximum load is approximately 77N. The grades of PZT fibers and epoxy resins used in manufacturing of MFCs could also be the reasons for the observed discrepancy in the ultimate stresses obtained in Williams' and our works. It should also be noted that in our experiments, the strain gauge readings vary between 0-75με and the load cell readings drift between 0-2N (~1MPa) in the unloaded condition.

The stress-strain behavior also shows noticeable dips above 1000με which are due to the formation of cracks. Once the cracks are formed, stress is reduced and increased again gradually indicating the hardening behavior. Several such trends can be easily observed in Figure 6(a), indicating the formation of multiple cracks. However, two specimens failed below 1000με without showing any strain hardening behavior. Multiple cracks on one of the tested specimens are shown in Figure 5(b), where the cracks are formed across the MFC, damaging both the PZT fibers and epoxy matrix. During the energy harvesting tests, the voltage output of PEH is reduced sharply at 6m/s^2 because of formation of cracks as the strain amplitude is much higher than 1000με (Figure 4). Though the MFCs withstood strains up to 4500με without fracture, it is obvious that their performance degrades even with the formation of a single crack. From Figure 6(a), 1000με can be considered as the upper limit of MFC for quasi-static loading conditions. It will be shown in the subsequent section through reliability tests that MFC shows appreciable degradation even at strains below 1000με under dynamic loading.

4. Reliability tests of macro fiber composite

In the previous section, the results of quasi-static tensile tests of MFC are shown. However, in actuator/sensor/harvester applications, the piezoelectric materials undergo dynamic loading. Fatigue failure due to cyclic stresses or strains on the materials is the cause for damage in more than 90% of mechanical structures [25]. In the context of present study, not only permanent damage or fracture in piezoelectric material, but considerable degradation in either mechanical or electrical response of piezoelectric material can be considered as failure. For example, 30% reduction in voltage output across the resistor load of PEH results in 51% drop in power output which might render harvester useless. Therefore, it is very important to understand the influence of dynamic loading on the performance of piezoelectric materials. To the best of authors' knowledge, neither previous works nor manufacturer's data sheet of MFC provide specific upper limit on dynamic stress or strain below which a high reliable performance is expected.

In this section, the results of reliability tests on PEHs are presented. It is very difficult to conduct conventional fatigue tests on thin piezoceramic patches where repeated cycles of axial tension-compression are applied. It is pointed out earlier that the piezoceramics normally exhibit higher compressive strength than tensile strength. However, as the size of specimen decreases, compressive load would lead to significant lateral movement of the specimen resulting in premature failure. It is worth mentioning that because of the susceptibility of thin PZT patches for failure in compression, most of the reliability tests conducted in previous studies used biased voltage which induced lower compressive stress when compared to tensile stress. For instance, an MFC which consists of 0.18μm thin PZT fibers embedded in epoxy matrix was reported to endure 2000με (peak to peak) [18]. However, the applied voltage on MFC actuator varied from -500V to 1500V which resulted in a state of strain approximately between -500με to 1500με. In the present study, PEHs are opted for investigating the reliability of MFC under complete reversed bending cycles. The PEHs were tested for long duration of time at different base accelerations corresponding to certain strain amplitudes and the responses were recorded continuously. All the tests were conducted at the initial resonant frequency of harvester corresponding to the base acceleration, i.e., the base excitation frequency did not change while the resonance of harvester slightly shifted in the course of testing due to material degradation. The typical operation frequency of piezoelectric harvesting applications ranges from 5 to 200Hz. Hence two sets of tests are conducted; one set with low resonant frequency around 30Hz and the other with high resonant frequency around 135Hz. The reliability tests conducted with low resonant frequency are carried out for 20 million cycles and those with high resonant frequency are carried out for 60 million cycles. The configuration of tested PEHs at low frequency for the performance evaluation of MFC is the same as the specimen used for energy harvesting tests (see Section 2). However, the tip mass was removed in the performance tests conducted at high frequency (~135Hz). All tests were conducted at experimentally determined optimal load resistances as shown in Figure 7. The optimal resistances values were 410kΩ and 82kΩ at the low and high frequencies, respectively. Although the aluminum beam and MFC dimensions were the same for both cases, the presence/absence of tip mass influenced the optimal resistance value as shown in the figure.

The results of first set of experiments carried out at low resonant frequencies (~30Hz) are plotted in Figure 8. The voltage responses of ten PEHs tested over 20 million cycles at various base accelerations are plotted in the figure. Two specimens were tested at each base acceleration for better understanding of material behavior and to reduce the margin of error in the findings. The resonant frequencies of tested harvesters varied between 29Hz to 31.1Hz depending on the base acceleration and also because of slight variation in specimen preparation. From Figure 8(a), it is clear that the harvesters did not show any signs of degradation in the voltage output at $1m/s^2$ and $2m/s^2$ with strain amplitudes below 600με. However, the voltage output from two harvesters tested at base acceleration of $3m/s^2$ with strain amplitude of 765με shows significant dips, indicating possible formation of cracks. Although, the voltage output is recovered in both cases possibly due to closure of cracks but has shown continuous degradation over time in case of PEH-6. The harvesters' performance at $4m/s^2$ and $6m/s^2$ plotted in Figure 8(b) shows multiple dips and severe degradation as they were tested at high strain amplitudes more than 1000με. A significant decrease of 55% in the voltage output of PEH-10 was observed after 20 million cycles. At high strain amplitude, dips in voltage were observed much earlier (less than 2 million cycles), indicating the early formation of cracks. The performance degradation of harvesters tested at high strain amplitude also indicates change in resonant frequency as observed in Figure 4(b). The observed drift in resonant frequency during the operation of harvester is not acceptable as it may result in significant power loss. Though few active tuning techniques have been proposed in the literature, none of them are feasible as they dissipate most or all of the harvested power [2]. Hence degradation in voltage output and change in resonant frequency are considered as potential failures. From the results presented in Figure 8(a) and 8(b), it can be concluded that the performance of MFC is affected considerably beyond strain amplitude of 750με.

The reliability of MFC performance was further investigated at high frequency to understand the influence of high strain rate. The same harvester configuration as in the previous tests is used without the tip mass, which possesses a high resonant frequency of about 135Hz. Degradation was observed around strain amplitude of 750μϵ in the previous tests conducted at low resonant frequencies. So, two tests are conducted at high frequency; one with 605μϵ and the other with 825μϵ of strain amplitude on MFC. The strain gauge data from two tests is plotted in Figure 9. The strain amplitude of 560μϵ was obtained on the MFC of PEH-11 at resonant frequency of 136.9Hz under base acceleration of 2.69g and the corresponding maximum strain on the MFC is 605μϵ. High strain amplitude of 765μϵ on PEH-12 was attained at 132.6Hz under base acceleration of 4.31g and its corresponding maximum strain is 825μϵ. The mean strain should be zero as these two harvesters do not have any tip mass. But small mean strain can be observed in Figure 9 due to experimental error which is unavoidable. Note that the resonant frequencies for the above two cases are slightly apart just because of variation in specimen preparation.

Higher base accelerations were used in the tests conducted at high frequencies when compared to tests conducted at low frequencies. It is because the amplitude of vibration decreases with increasing resonant frequency for a constant base acceleration and vice-versa. Hence, high base accelerations are required to achieve sufficient amplitude to induce high strains on MFC. It is worth mentioning that, such high base accelerations are not practically available; they were used in the present study to understand the influence of high strain rate. The voltage and tip displacement were recorded for almost 60 million cycles which is approximately six days of testing. The voltage and tip displacement are normalized with their initial values and plotted in Figure 10. The results of PEH-11 with maximum strain of 605μϵ show reliable performance over the duration of testing with ±3% variations of mean values. No significant degradation in performance is observed during the entire testing period. However, the performance of PEH-12 under higher strain amplitude (825μϵ) shows steady decline over the time because of material degradation. When the PEH is operated at high strain amplitudes, the stiffness of MFC decreases over time because of formation of cracks, and consequently the resonant frequency of PEH reduces. When the resonant frequency reduces with time, the mismatch between the resonant frequency and excitation frequency increases as the excitation frequency is kept constant during testing. As the harvester is operated gradually farther away from its resonant frequency, its voltage output and tip displacement steadily decrease. Approximately 15% reduction in voltage output is observed after 55 million cycles which results in 28% drop in the harvested power. These results are analogous to the trends observed in the previous tests conducted at low frequency, indicating that the frequency does not have significant effect on the fatigue behavior of MFC at least within the range considered in this work. The strain data is not recorded as the durability of strain gauges cannot be as high as 60 million cycles. The images of cracks induced in the MFC specimens during reliability tests are captured using a scanning electron microscope, as shown in Figure 11. The protective polyimide film on the specimen is removed and a thin layer of platinum (in order of nm) is coated. The cracks shown in Figure 11(a), (b) and (c) are captured at 100x, 500x and 5000x magnification, respectively. The cracks are formed perpendicular to the axial direction because of high strains induced in MFC and the cyclic nature of strain due to the dynamic motion of harvester further assists in crack propagation. The parallel slots visible in Figure 11(a) are imprints of interdigitated electrodes sandwiched between PZT fibers and polyimide film. One or more cracks are observed when the MFC was tested above strain amplitude of 700μϵ. From these results, it can be concluded that the MFC shows high reliable performance under completely reversed strain amplitudes below 600μϵ only. The strain gauges were bonded with slight misalignment but the error in angle is smaller than 5^0. The images of specimens are captured at magnification of 20x (Figure 5(b)) and hence the slight misalignment appears amplified. The principle strain direction is along the length of beam (ϵ_1) with zero strain in the width direction (ϵ_2). Assuming 5^0 misalignment in bonding, the error in the measured strain is $1/\cos 5^0 - 1 = 0.0038$, which is ~4ppm out of 1000ppm measured strain. Therefore, the error in strain measurement due to misalignment in bonding can be neglected.

The MFC supplier's data sheet specifies 4500με as the maximum operational tensile strain. However, it is found in the present study that formation of cracks in MFC is initiated as early as 1000με during the tensile tests. Moreover, it is observed that high reliable performance of MFC can only be achieved under completely reversed strain amplitude of 600με for energy harvesting applications. Thus, a dynamic strain limit of 600με is proposed here for MFC, which can be used in the design of MFC based PEHs for practical applications. In this study, approximately 100 days were spent to carry out tests on MFC for evaluating its reliability at various strain amplitudes and two different frequencies.

It is a common practice to use a factor of safety in engineering designs, which is a ratio of material failure limit to the actual stress or strain in the material. The use of factor of safety in designing PEHs will provide sufficient margin between operating strain on harvester and the dynamic strain limit, thus ensuring very reliable operation. The proposed dynamic strain limit is also applicable to MFC bending actuators undergoing completely reversed strains. It should be ensured that the applied electric fields to the actuators do not induce strain in excess of 600με. Similar studies on other piezoelectric materials like PMN-PT, PVDF and $BaTiO_3$ shall be performed to ascertain their dynamic strain limits for designing reliable PEHs in practical applications.

5. Conclusions

This paper investigated the reliability of MFC at various strain amplitudes under reversed loading as found in energy harvesting applications. Firstly, energy harvesting tests are carried out on a PEH comprising MFC, and significant shift in resonant frequency of PEH is observed for strains below 1000με. Moreover, more than 50% degradation in voltage output within half million cycles is noticed at strain amplitude around 1370με. Later, tensile tests are carried out on the MFC and the nonlinear stress-strain behavior below 1000με is obtained, which is responsible for the observed drop in resonant frequency with increasing strain amplitude in the energy harvesting tests. These results indicate that the MFC does not have a clear linear elastic limit. In addition, it is noticed from the tensile tests that crack formation is initiated in the MFC at strains as low as 1000με. Finally, several long duration reliability tests are conducted at both low and high resonant frequencies to estimate the upper limit of dynamic strain in the MFC, below which the material gives reliable performance. It is concluded that the MFC gives high reliable performance under dynamic strain of 600με and does not show any degradation in voltage output and tip displacement over 60 million cycles of testing. The results of reliability tests also indicate that the frequency considered in typical energy harvesting applications does not have significant effect on the fatigue behavior of MFC.

Funding Acknowledgements

The authors gratefully acknowledge the funding support from Office of Naval Research, Washington, DC, under the grant no. N62909-13-1-N202.

Notes

I. Smart materials. Properties of MFC patch available at : http://www.smart-material.com/MFC-product-main.html (accessed on 9 February 2016)

II. MIDE Volture. Properties of PZT wafer available at :

http://www.mide.com/collections/piezoelectric-products (accessed on 9 February 2016)

III. Morgan Advanced Materials. Properties of PZT bimorph available at : http:// www.morganelectroceramics.com/products/piezoelectric/piezo-bimorphs/r6001_piezo _brochureweb.pdf (accessed on 9 February 2016)

IV. Channel Industries, Inc. Properties of PZT patch available at : http://www.channeltechgroup.com/products-and-services/piezoelectric-materials/ceramics (accessed on 9 February 2016)

V. http://www.matweb.com/search/QuickText.aspx?SearchText=AL%206061%20T6 (accessed on 9 February 2016)

VI. http://www.matweb.com/search/QuickText.aspx?SearchText=230%20BRASS%20H08 (accessed on 9 February 2016)

VII. http://www.matweb.com/search/QuickText.aspx?SearchText=AISI%201050%20Steel%2C%20as%20rolled (accessed on 9 February 2016)

References

1. Cook-Chennault KA, Thambi N and Sastry AM 2008 Powering MEMS portable devices—a review of non-regenerative and regenerative power supply systems with special emphasis on piezoelectric energy harvesting systems *Smart Materials and Structures* **17(4)** 043001
2. Toprak A and Tigli O 2014 Piezoelectric energy harvesting: State-of-the-art and challenges *Applied Physics Reviews* **1(3)** 031104
3. Sodano H, Park G and Inman D 2004 Estimation of electric charge output for piezoelectric energy harvesting *Strain* **40(2)** 49–58
4. Erturk A and Inman D J 2008 A distributed parameter electromechanical model for cantilevered piezoelectric energy harvesters *Journal of Vibration and Acoustics* **130(4)** 041002
5. Arafa M, Akl W, Aladwani A, Aldraihem O and Baz A 2011 Experimental implementation of a cantilevered piezoelectric energy harvester with a dynamic magnifier *Proceedings of SPIE* pp. 79770Q-79770Q
6. Abdelkefi A, Barsallo N, Tang L, Yang Y and Hajj M R 2013 Modeling, validation, and performance of low-frequency piezoelectric energy harvesters *Journal of Intelligent Material Systems and Structures* **25(12)** 1429–1444
7. Tang L, Yang Y and Soh CK 2010 Toward broadband vibration-based energy harvesting *Journal of Intelligent Material Systems and Structures* **21** 1867-1897
8. Anton SR, Erturk A and Inman DJ 2010 Strength analysis of piezoceramic materials for structural considerations in energy harvesting for UAVs *In Proceedings of SPIE Vol* **7643** pp. 76430E-76430E
9. Shafer MW and Garcia E 2014 The power and efficiency limits of piezoelectric energy harvesting *Journal of Vibration and Acoustics* **136(2)** 021007
10. Upadrashta D, Yang Y and Tang L 2014 Material strength consideration in the design optimization of nonlinear energy harvester *Journal of Intelligent Material Systems and Structures* **26(15)** 1980-1994
11. Lupascu, D and Rödel J 2005 Fatigue in bulk lead zirconate titanate actuator materials. *Advanced Engineering Materials* **7(10)** 882-898
12. Mall S and Hsu TL 2000 Electromechanical fatigue behavior of graphite/epoxy laminate embedded with piezoelectric actuator *Smart Materials and Structures* **9(1)** 78

13. Yocum M, Abramovich H, Grunwald A and Mall S 2003 Fully reversed electromechanical fatigue behavior of composite laminate with embedded piezoelectric actuator/sensor *Smart materials and structures* **12(4)** 556
14. Chaplya PM, Mitrovic M, Carman GP and Straub FK 2006 Durability properties of piezoelectric stack actuators under combined electromechanical loading *Journal of applied physics* **100(12)** 124111
15. Wang H, Wereszczak AA and Lin H T 2009 Fatigue response of a PZT multilayer actuator under high-field electric cycling with mechanical preload *Journal of applied physics* **105(1)** 014112
16. Wang H, Matsunaga T, Lin H T and Mottern A M 2012 Piezoelectric and dielectric performance of poled lead zirconate titanate subjected to electric cyclic fatigue *Smart Materials and Structures* **21(2)** 025009
17. Bhattacharyya M and Arockiarajan A 2013 Electrical fatigue behaviour in lead zirconate titanate: an experimental and theoretical study *Smart Materials and Structures* **22(8)** 085032
18. Wilkie WK, High J and Bockman J 2002 Reliability testing of NASA piezocomposite actuators *In Proceedings of the 8th International Conference on New Actuators* pp. 10-12
19. Tarazaga PA, Inman DJ and Wilkie WK 2007 Control of a space rigidizable inflatable boom using macro-fiber composite actuators *Journal of Vibration and Control* **13(7)** 935-950
20. Discalea FL, Matt H, Bartoli I, Coccia S, Park G and Farrar C 2007 Health monitoring of UAV wing skin-to-spar joints using guided waves and macro fiber composite transducers *Journal of intelligent material systems and structures* **18(4)** 373-388
21. Fett T, Muller S, Munz D and Thun G 1998 Nonsymmetry in the deformation behaviour of PZT *Journal of Materials Science Letters* **17(4)** 261-265
22. Stanton SC, Erturk A, Mann BP, Dowell EH and Inman DJ 2012 Nonlinear nonconservative behavior and modeling of piezoelectric energy harvesters including proof mass effects *Journal of intelligent material systems and structures* **23(2)** 183-199
23. Abdelkefi A, Nayfeh AH, Hajj MR 2012 Global nonlinear distributed-parameter model of parametrically excited piezoelectric energy harvesters *Nonlinear Dynamics* **67(2)** 1147-1160
24. Williams RB, Inman DJ, Schultz MR, Hyer MW and Wilkie WK 2004 Nonlinear tensile and shear behavior of macro fiber composite actuators *Journal of Composite Materials* **38(10)** 855-869
25. Vassilopoulos A P (Ed.) 2010 Fatigue life prediction of composites and composite structures. Elsevier.

Figure captions

Figure 1. (a) Schematic representation of cantilever type PEH (b) Experimental set up of energy harvesting tests.

Figure 2. Experimental responses of PEH for accelerations ranging from $1m/s^2$ to $6m/s^2$ (a) RMS voltage response across resistor (b) Maximum strain measured on MFC.

Figure 3. (a) Finite element model of PEH (b) Strain variation on the harvester materials due to weight of tip mass.

Figure 4. Variation of PEH response over time at base acceleration $6m/s^2$ (a) RMS voltage (b) Strain and resonant frequency.

Figure 5. (a) MFC with bonded strain gauge used for tensile tests (b) Multiple cracks across MFC specimen observed after tensile test.

Figure 6. (a) Experimental data of stress-strain behavior of MFC obtained from tensile tests and polynomial fit of data (b) Variation of stress and elastic modulus with strain.

Figure 7. Variation of power output with load resistance for performance evaluation tests carried out at low and high frequencies.

Figure 8. Reliability tests for performance evaluation of harvesters at different base accelerations at low resonant frequency (~30Hz) (a) $1m/s^2$, $2m/s^2$ and $3m/s^2$ (b) $4m/s^2$ and $6m/s^2$. Measured maximum strain on MFC for each specimen is mentioned in micro strain ($\mu\epsilon$).

Figure 9. Measured strain on MFCs of PEH-11 and PEH-12 during reliability tests at high resonant frequencies.

Figure 10. Normalized voltage and displacement responses of PEH-11 and PEH-12 harvesters tested at high resonant frequency. Measured maximum strain on MFC for each specimen is mentioned in micro strain ($\mu\epsilon$).

Figure 11. Microscopic images of cracks induced in MFC specimens during reliability tests. Figures (a), (b) and (c) are captured at 100x, 500x and 5000x magnification, respectively.

Biography

Mr. Deepesh Upadrashta was born in Visakhapatnam, India, in 1985. He graduated from Andhra University, India with a B.E. degree in Mechanical engineering in 2006. He received M.E. degree in Mechanical engineering from Indian Institute of Science, Bangalore, India in 2008. He is currently pursuing Ph. D. degree in structures and mechanics in School of Civil and Environmental Engineering, Nanyang Technological University, Singapore. His main research interests include energy harvesting, smart materials and structures and nonlinear dynamics.

Dr. Yaowen Yang is currently an Associate Professor in Nanyang Technological University (NTU), Singapore. His research interests include smart materials for energy harvesting, structural health monitoring and vibration control. Over the years, Dr Yang has received more than $3M research fund from funding agencies and industry, and published 1 book, 3 monographs and over 160 journal and conference papers. Dr Yang received his B.Eng and M.Eng from Shanghai Jiao Tong University and Ph.D from Nanyang Technological University. He serves as an editorial board member of a few international journals and a member of ASME technical committee on energy harvesting.

fig 1a

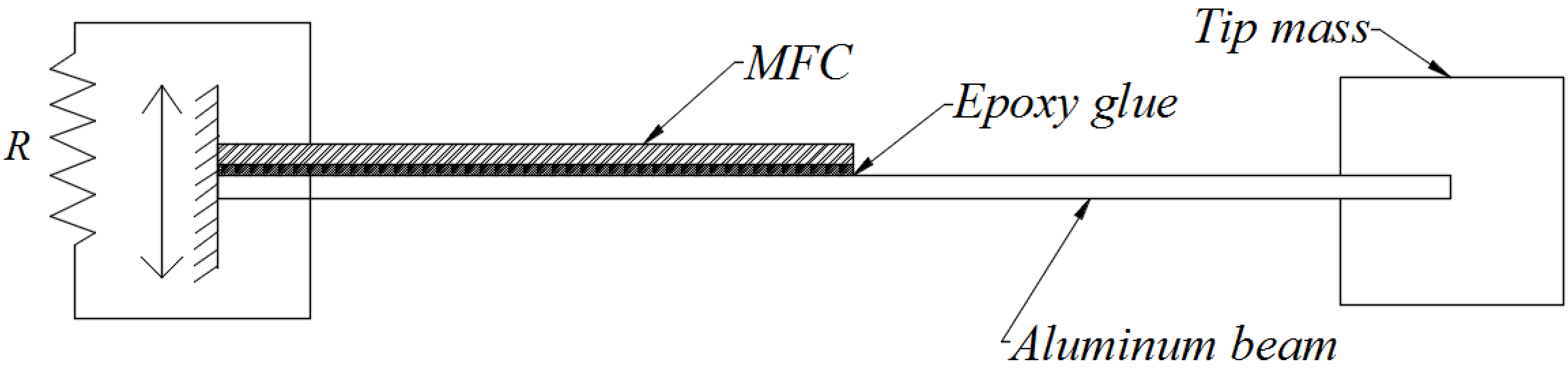

fig 1b

fig 2a

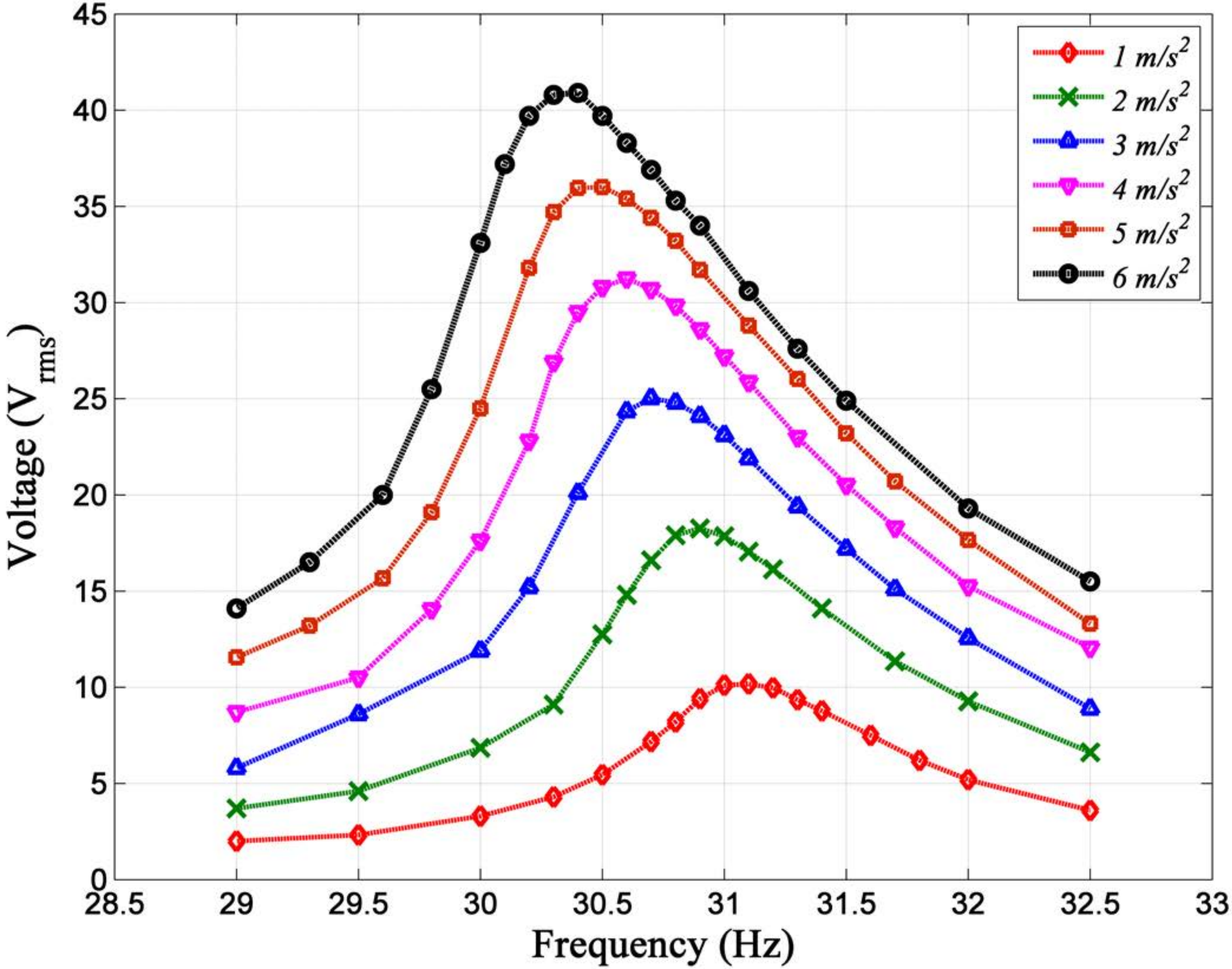

fig 2b

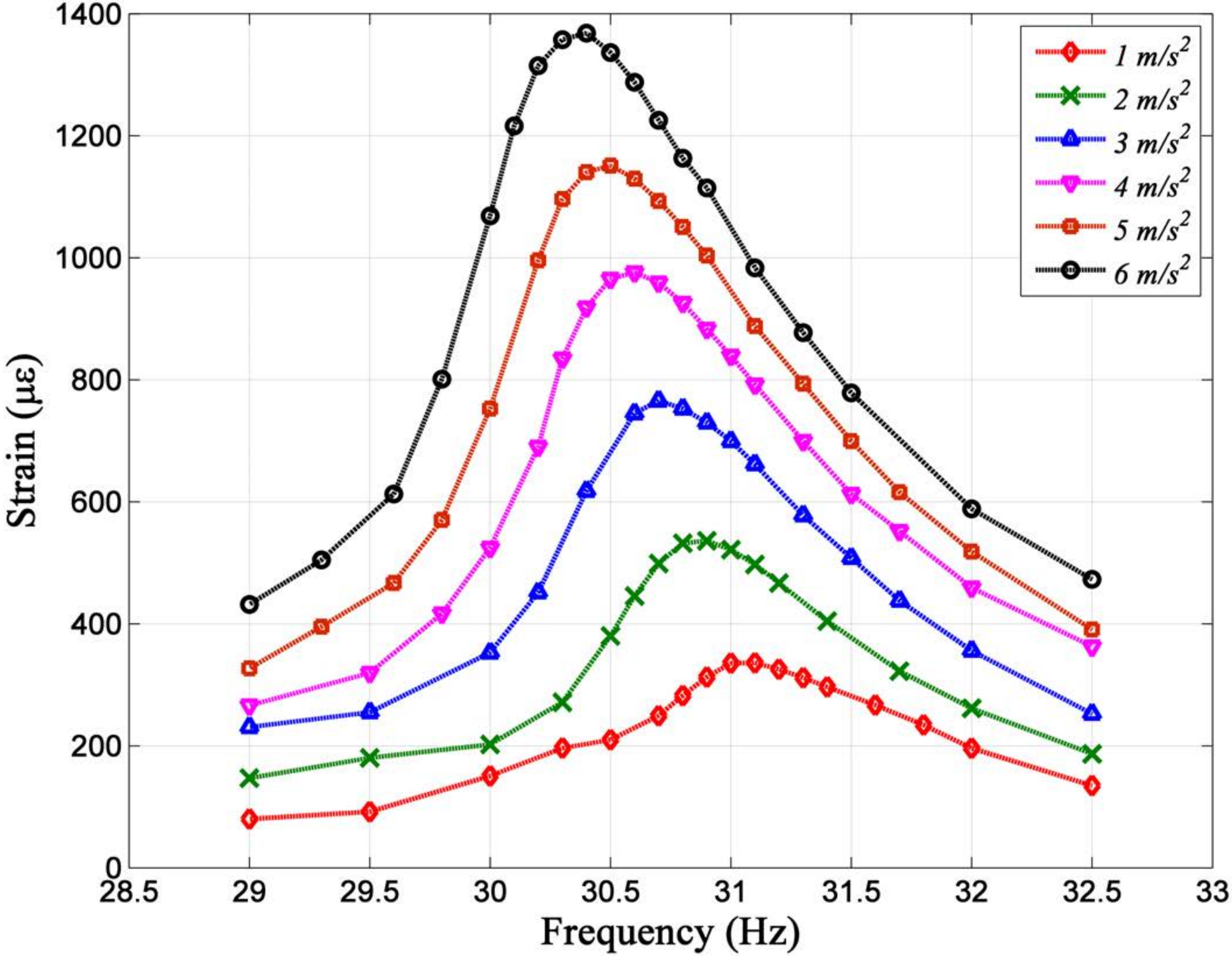

1400
1200
1000
800
600
400
200
0
28.5
29
29.5
30
30.5
31
31.5
32
32.5
33
Strain (με)
Frequency (Hz)
1 m/s2
2 m/s2
3 m/s2
4 m/s2
5 m/s2
6 m/s2

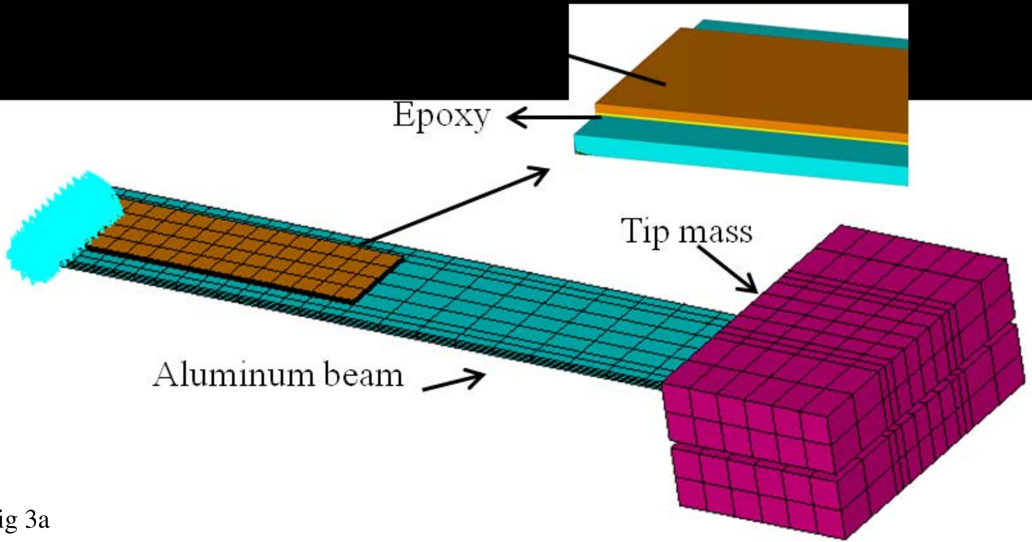

fig 3a

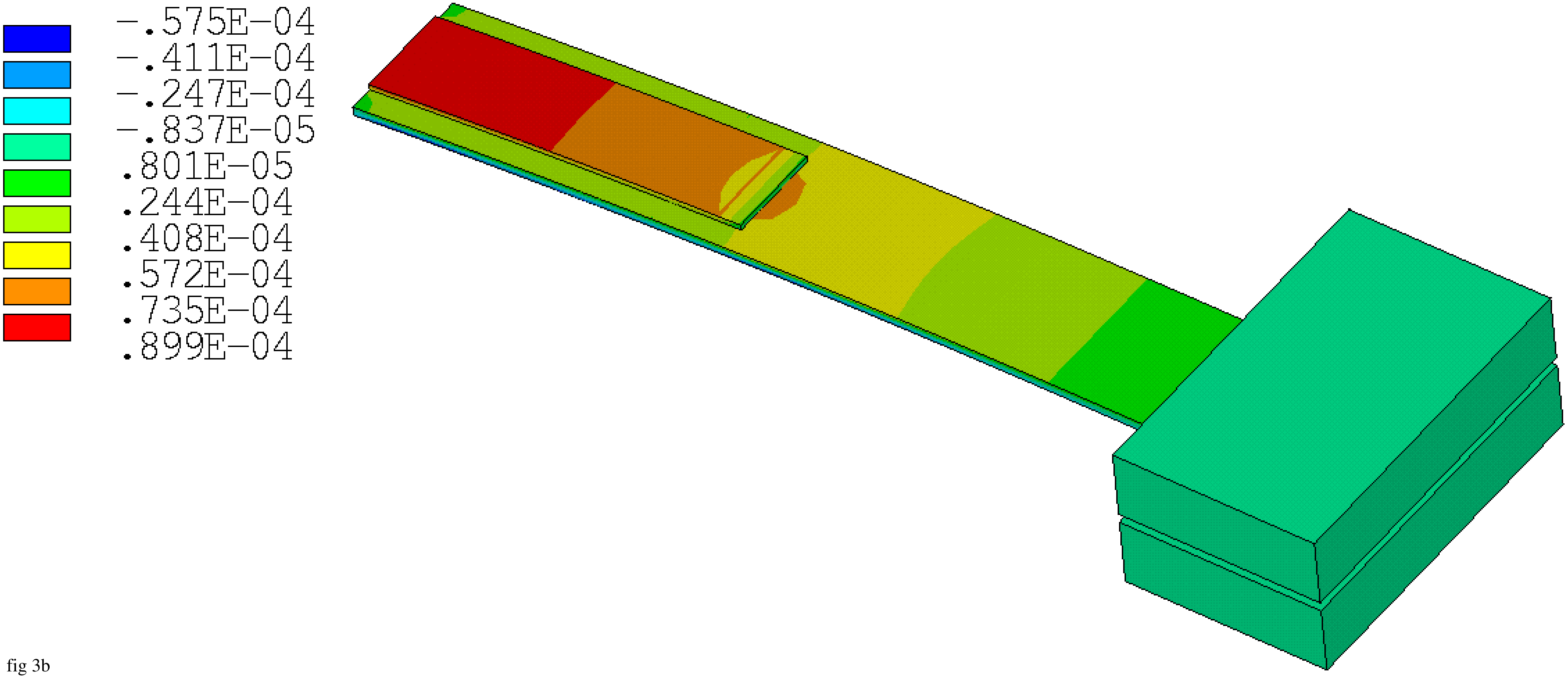
-.575E-04
-.411E-04
-.247E-04
-.837E-05
.801E-05
.244E-04
.408E-04
.572E-04
.735E-04
.899E-04

fig 3b

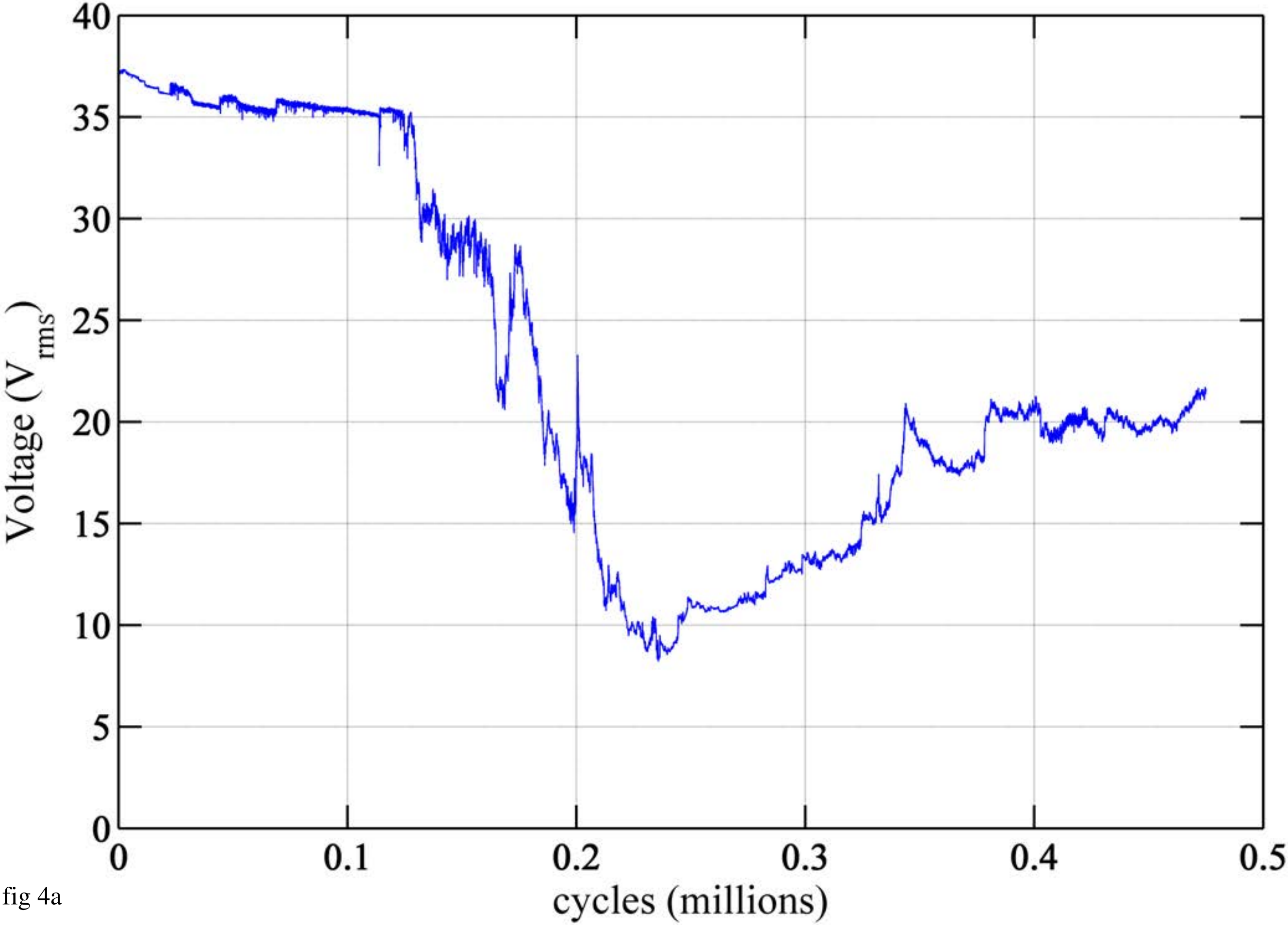

40
35
30
25
20
15
10
5
0
Voltage (V_{rms})
0
0.1
0.2
0.3
0.4
0.5
cycles (millions)

fig 4a

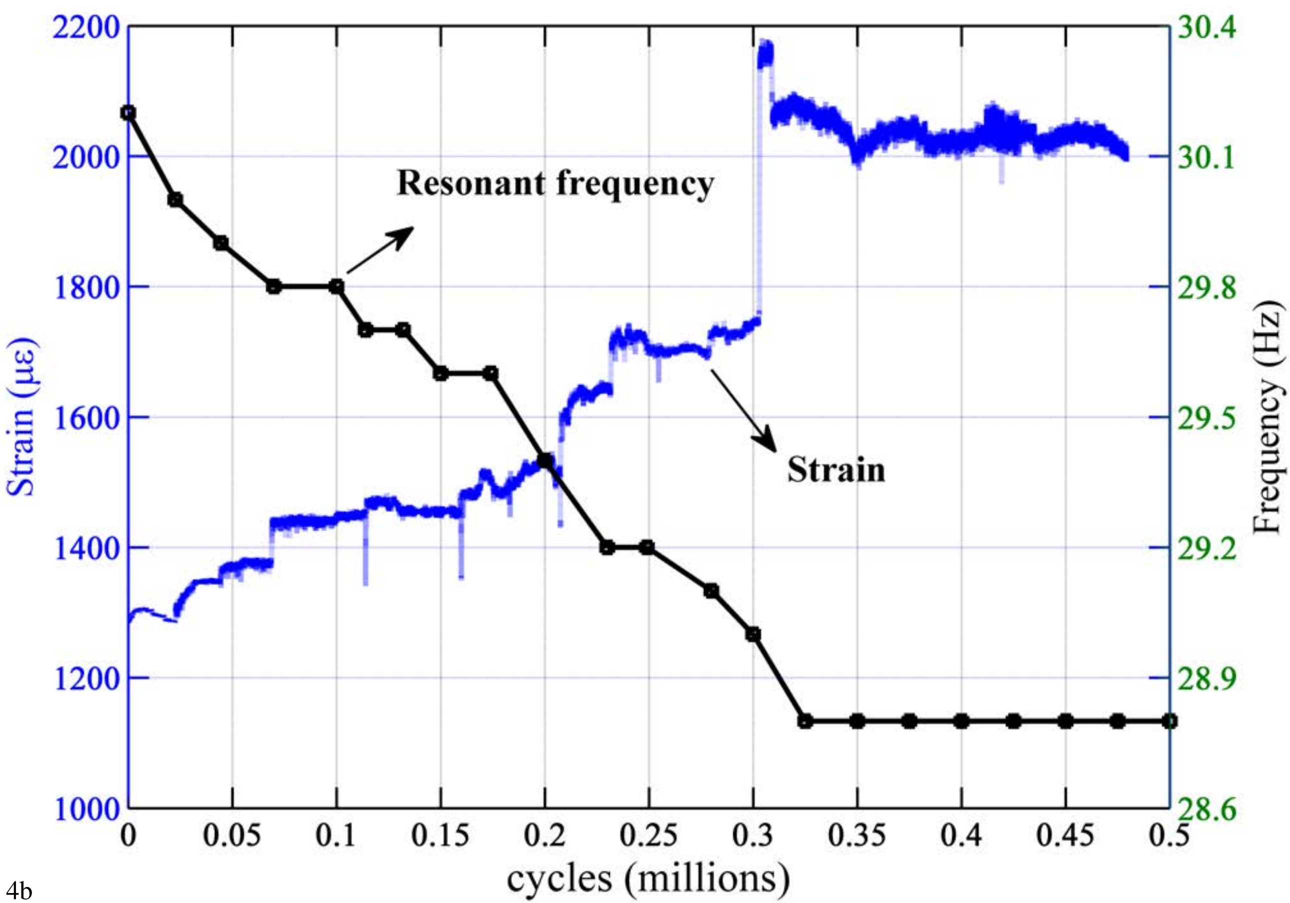

Resonant frequency
Strain
Strain (με)
Frequency (Hz)
cycles (millions)
2200
2000
1800
1600
1400
1200
1000
30.4
30.1
29.8
29.5
29.2
28.9
28.6
0
0.05
0.1
0.15
0.2
0.25
0.3
0.35
0.4
0.45
0.5

fig 4b

fig 5a

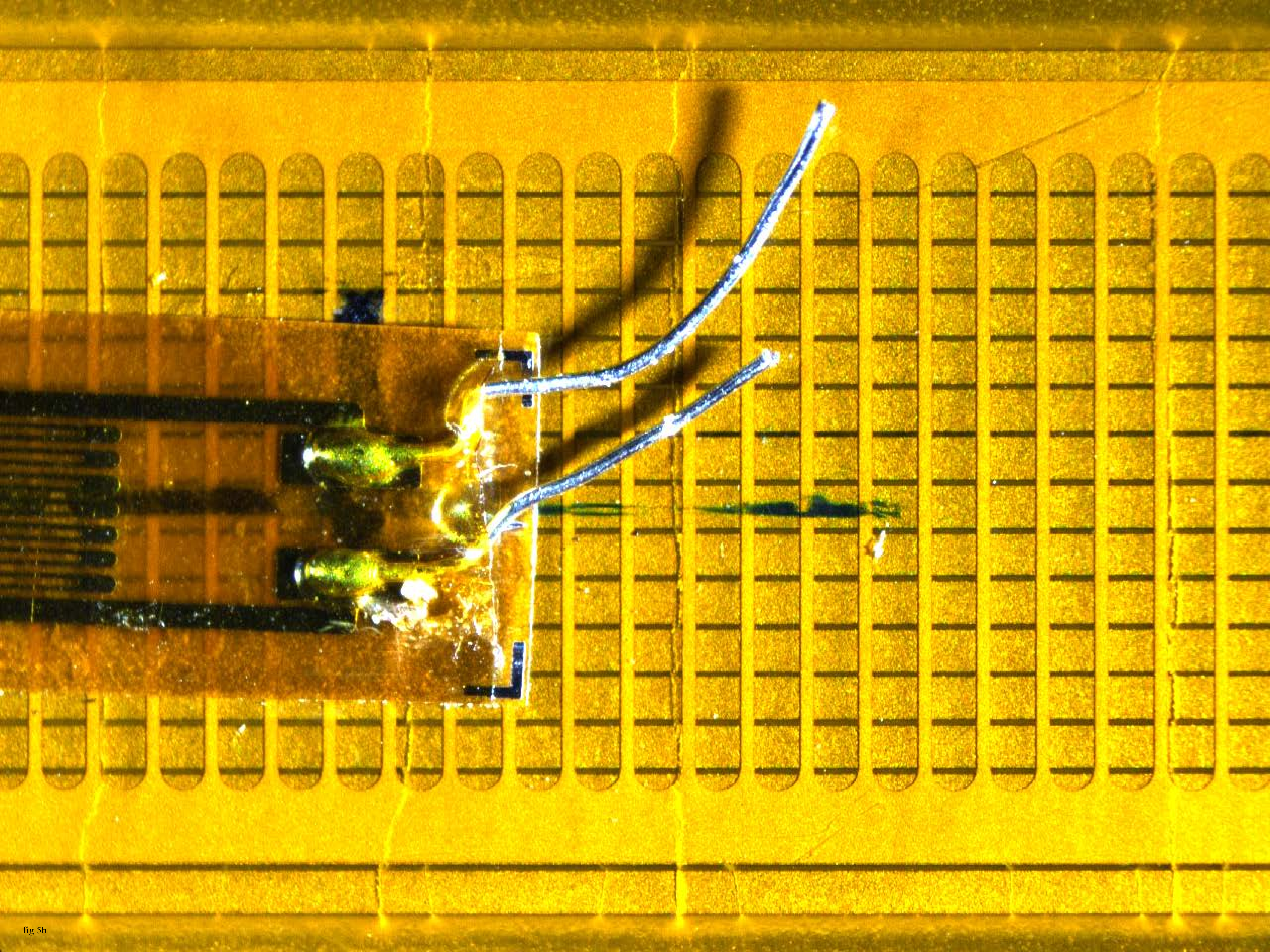

fig 5b

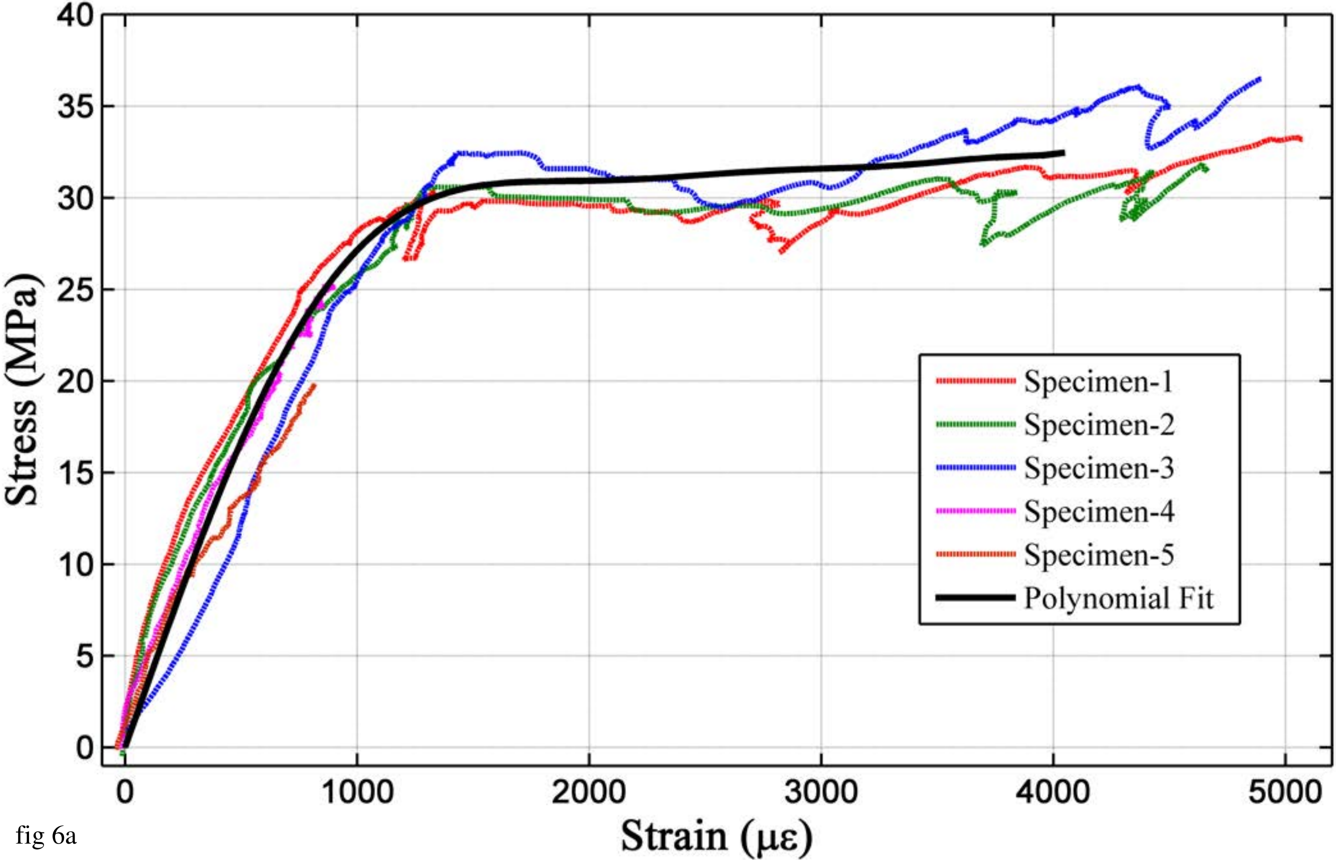

Stress (MPa)
Strain (με)
0
5
10
15
20
25
30
35
40
0
1000
2000
3000
4000
5000
Specimen-1
Specimen-2
Specimen-3
Specimen-4
Specimen-5
Polynomial Fit

fig 6a

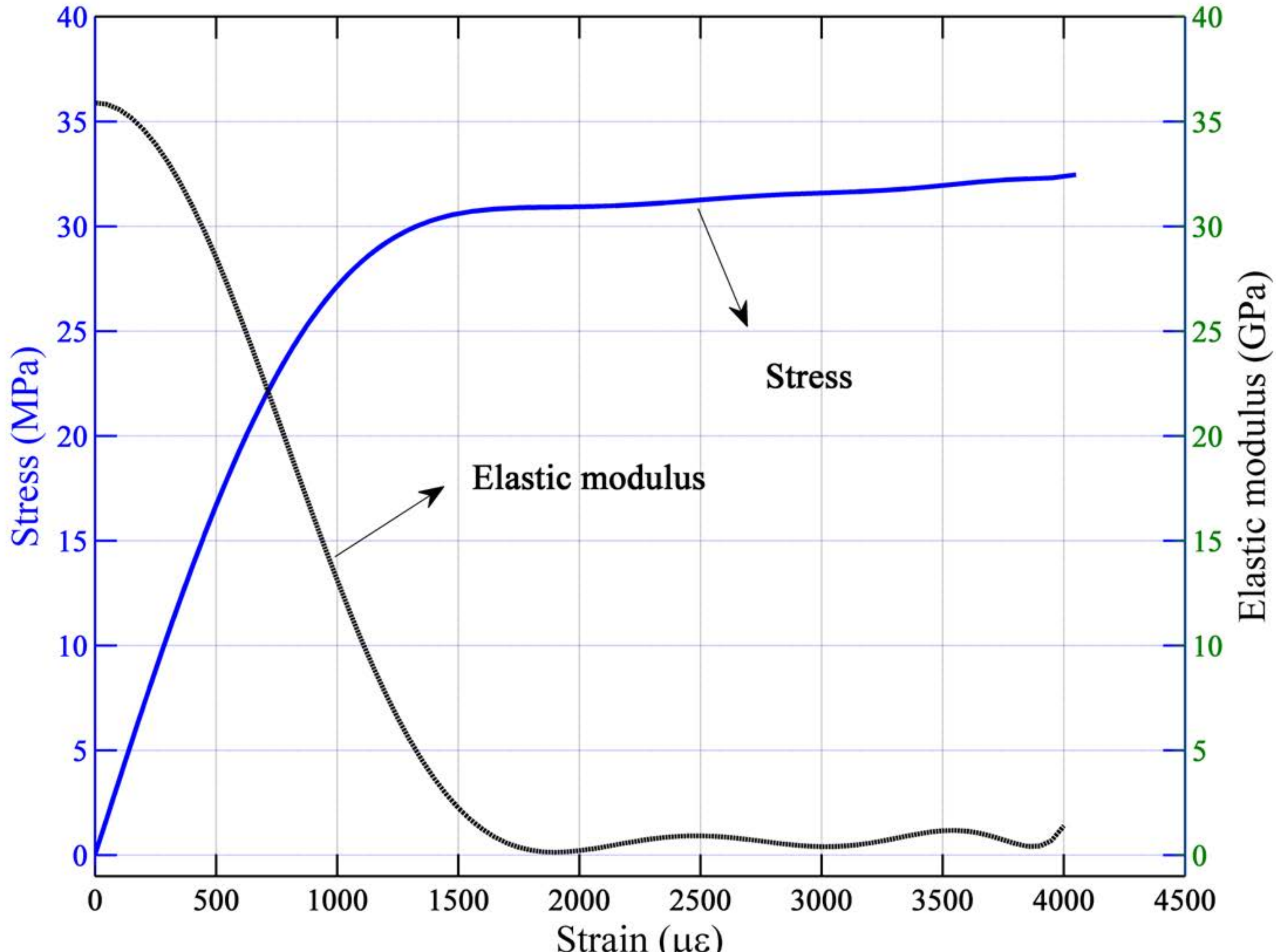

Stress (MPa)
Elastic modulus (GPa)
Strain (με)
Stress
Elastic modulus
0
5
10
15
20
25
30
35
40
0
500
1000
1500
2000
2500
3000
3500
4000
4500

fig 6b

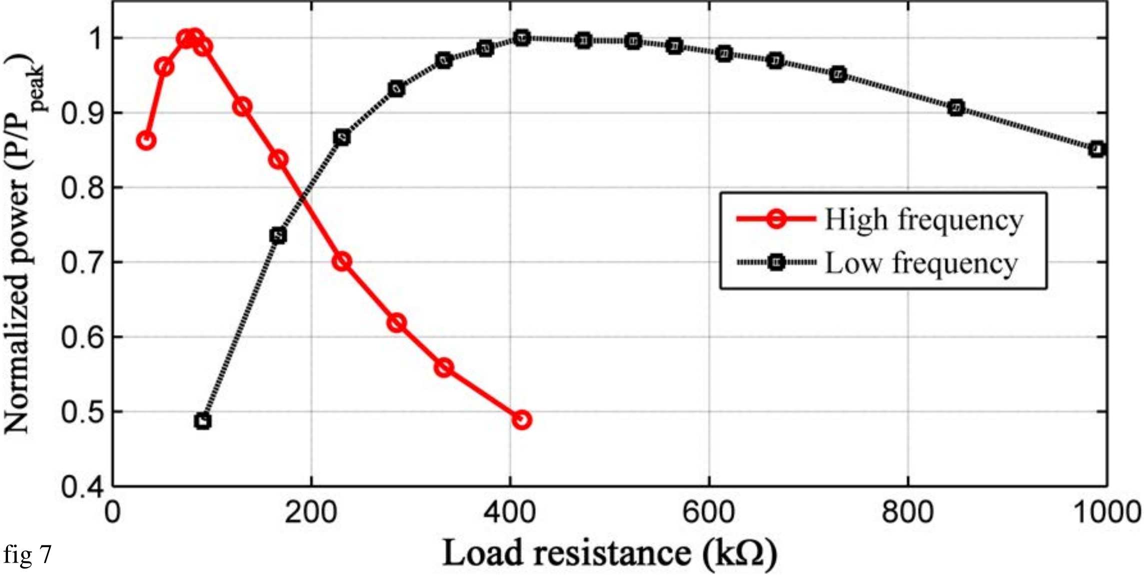
Normalized power (P/P_{peak})
1
0.9
0.8
0.7
0.6
0.5
0.4
0
200
400
600
800
1000
Load resistance (kΩ)
High frequency
Low frequency

fig 7

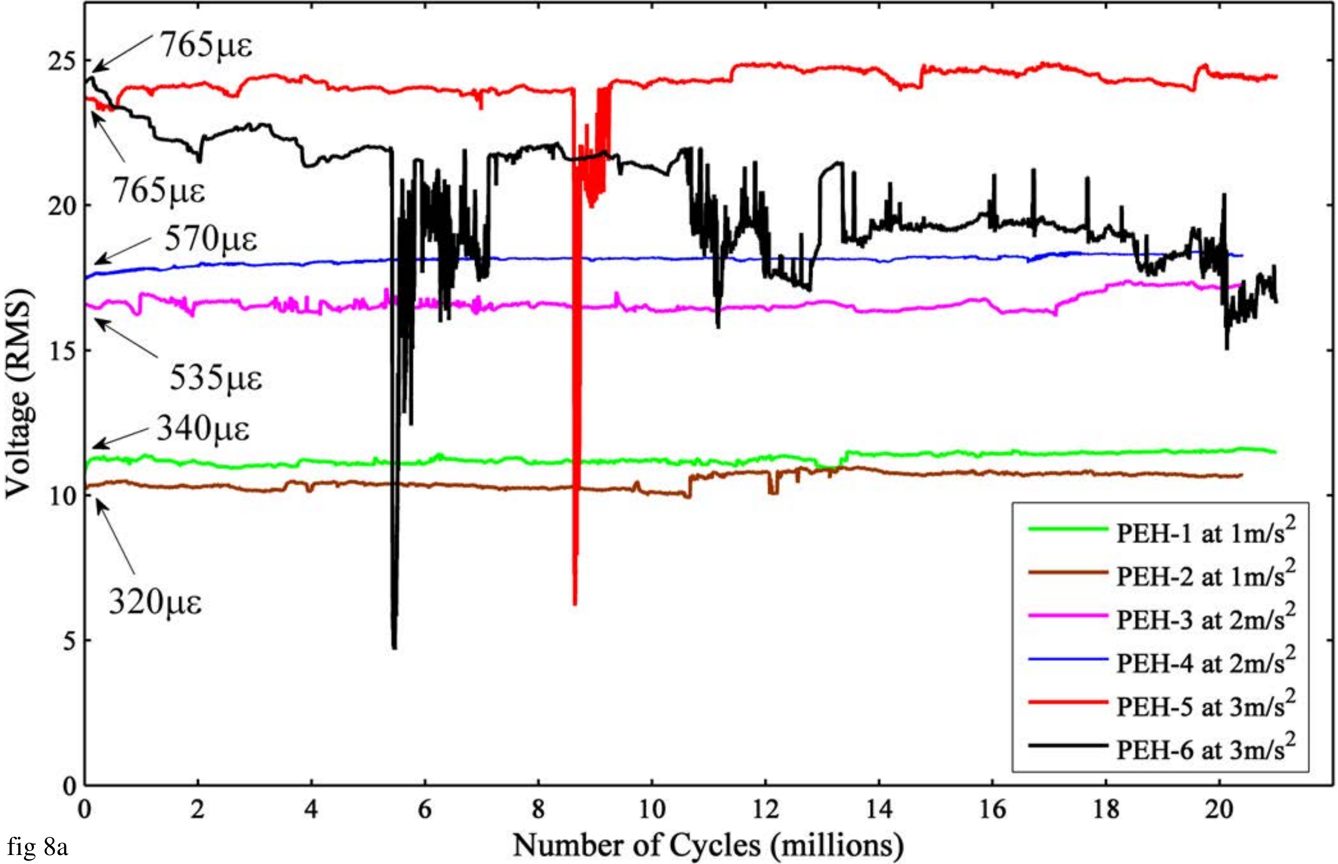
765με
765με
570με
535με
340με
320με
PEH-1 at 1m/s2
PEH-2 at 1m/s2
PEH-3 at 2m/s2
PEH-4 at 2m/s2
PEH-5 at 3m/s2
PEH-6 at 3m/s2
Voltage (RMS)
Number of Cycles (millions)
0
5
10
15
20
25
0
2
4
6
8
10
12
14
16
18
20

fig 8a

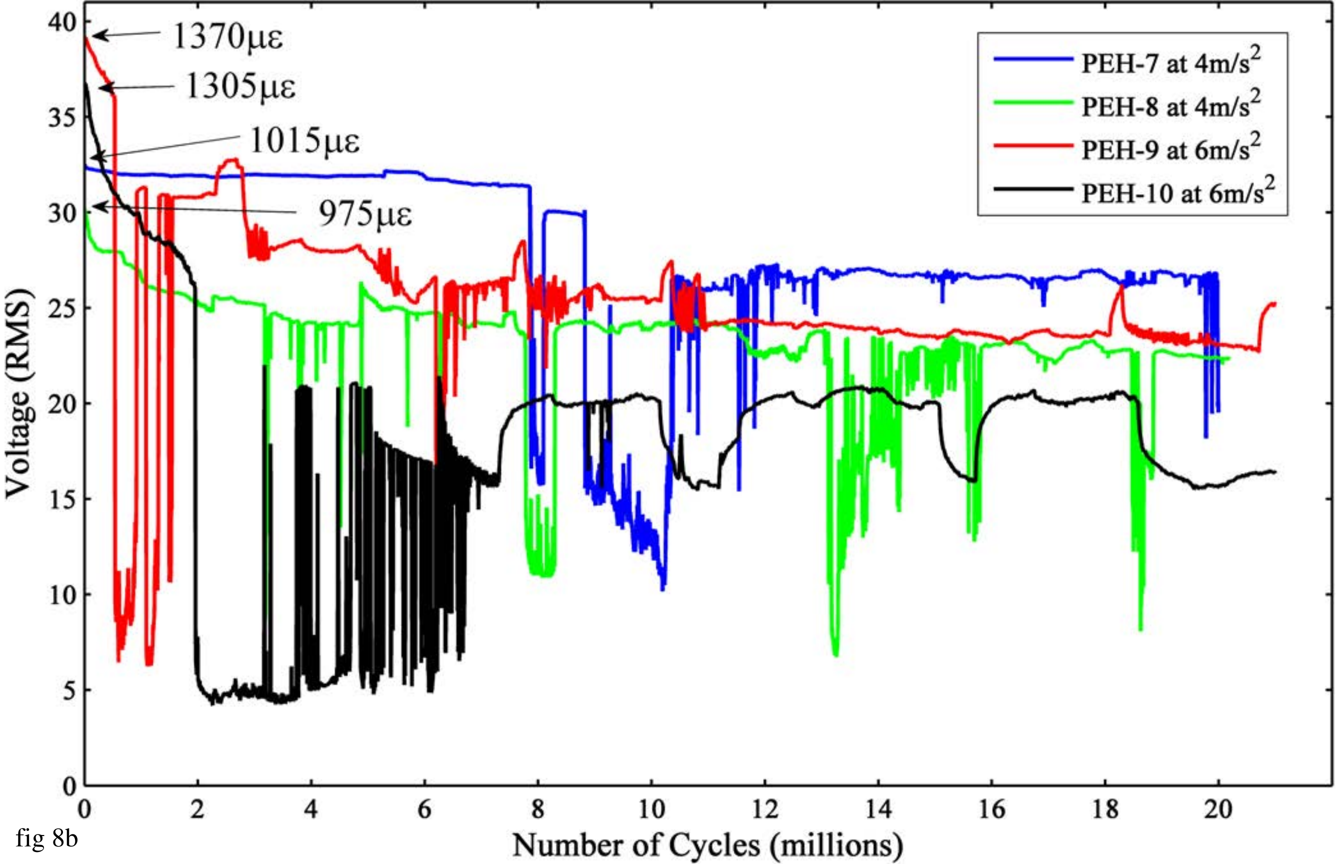
1370με
1305με
1015με
975με
PEH-7 at 4m/s2
PEH-8 at 4m/s2
PEH-9 at 6m/s2
PEH-10 at 6m/s2
Voltage (RMS)
Number of Cycles (millions)
0
5
10
15
20
25
30
35
40
0
2
4
6
8
10
12
14
16
18
20

fig 8b

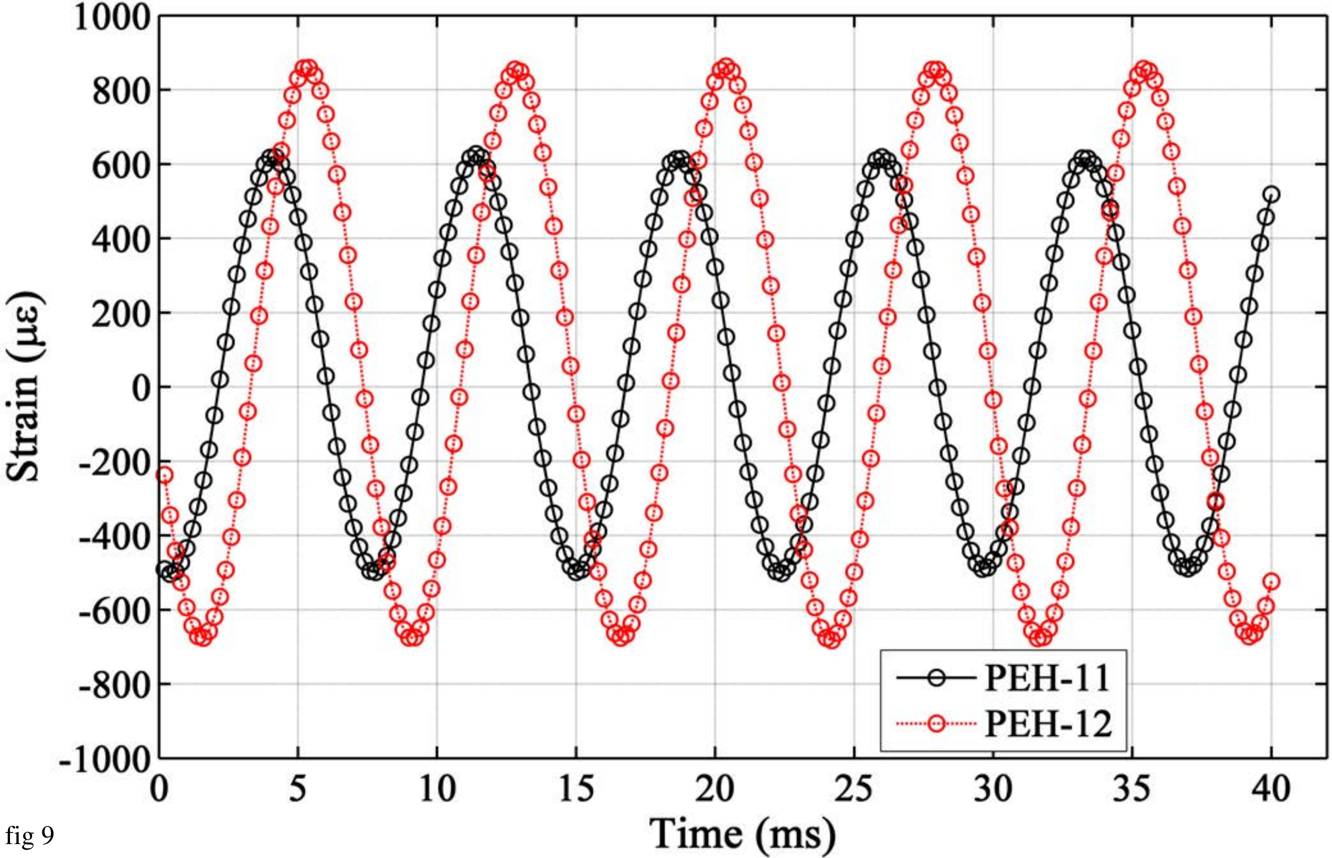
Strain (με)
Time (ms)
PEH-11
PEH-12
1000
800
600
400
200
0
-200
-400
-600
-800
-1000
0
5
10
15
20
25
30
35
40

fig 9

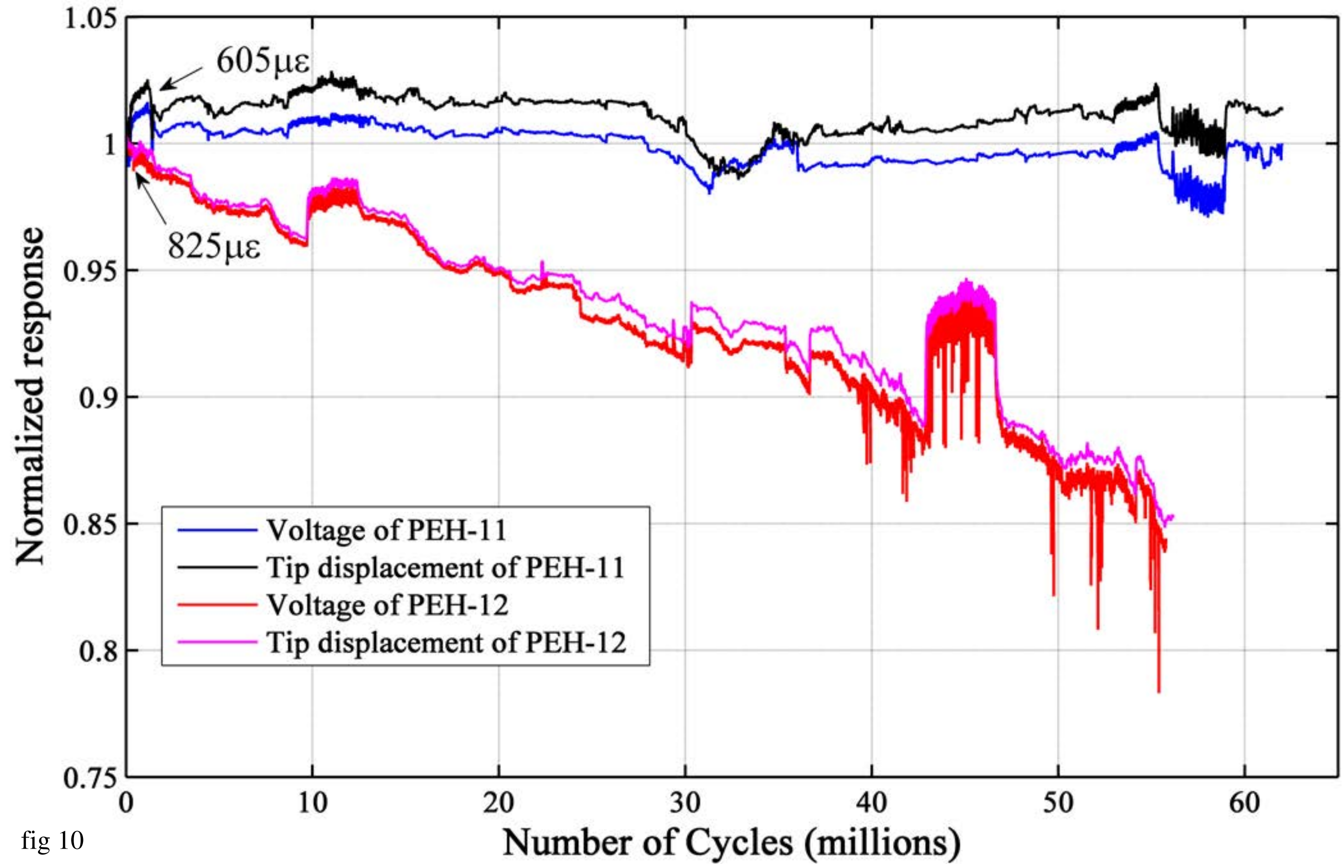
605με
825με
Voltage of PEH-11
Tip displacement of PEH-11
Voltage of PEH-12
Tip displacement of PEH-12
Normalized response
Number of Cycles (millions)
1.05
1
0.95
0.9
0.85
0.8
0.75
0
10
20
30
40
50
60

fig 10

fig 11a

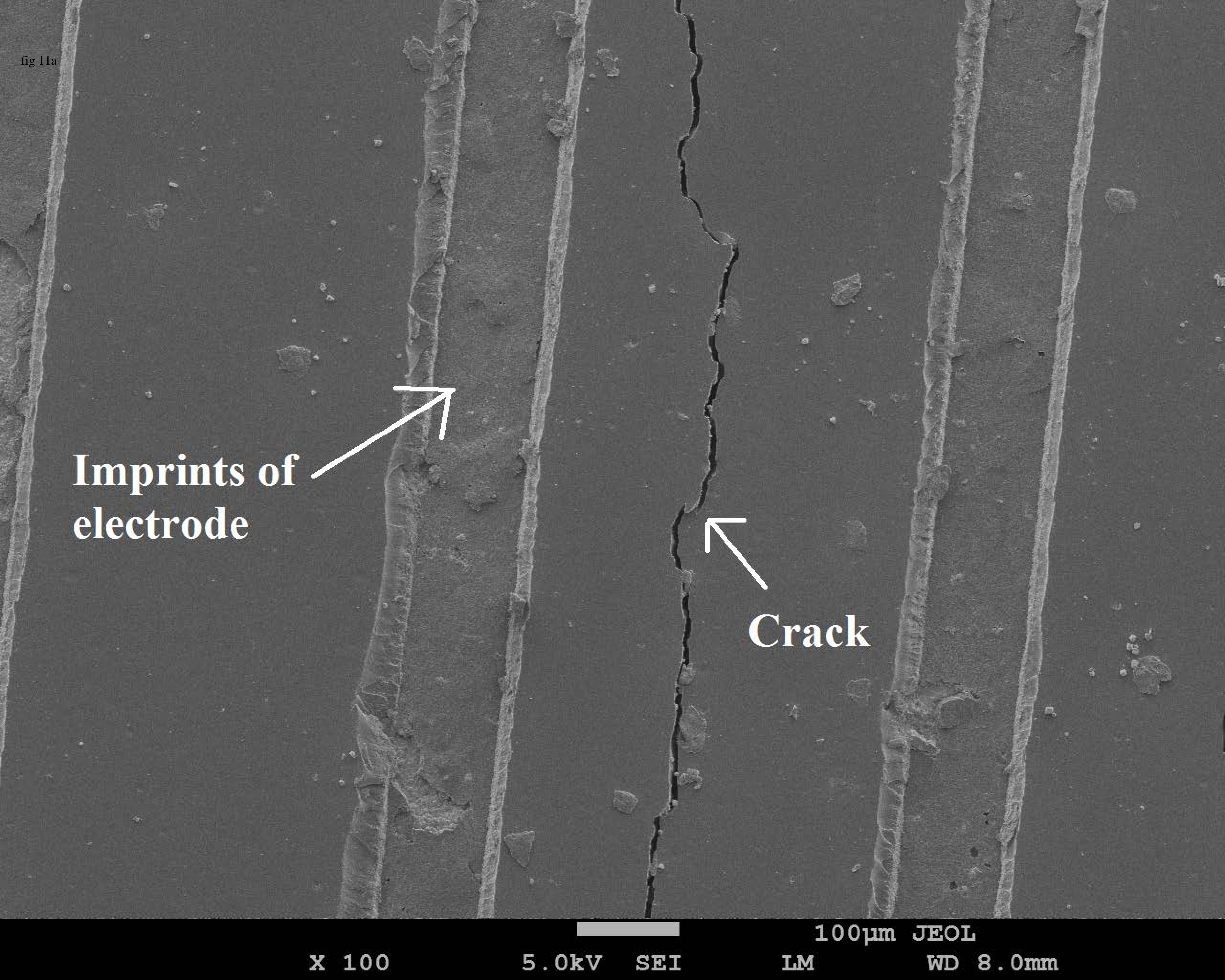
Imprints of
electrode
Crack
100µm JEOL
X 100
5.0kV
SEI
LM
WD 8.0mm

fig 11b

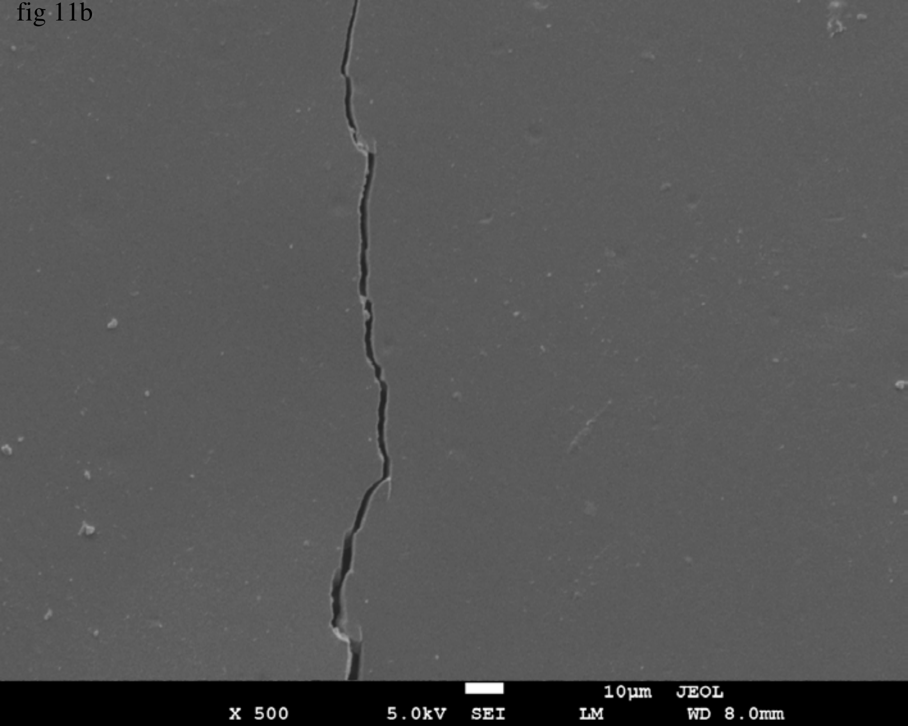

fig 11c